Final Report 01 Jan 92 - 31 Dec 93

DIELECTRIC LOADED BROADBAND GYRO-TWT SYSTEM

Professor N. C. Luhmann, Jr

Dept of Applied Science & Electrical & Computer Engrg
University of California
Davis, CA 95616

F49620-92-J-0175

AFOSR-TR- 94 0136

AFOSR/NE
110 Duncan Avenue, Suite B115
Bolling AFB DC 20332-0001

2301/ES

UNLIMITED

Basic research studies on the generation of high frequency waves at high power, while minimizing problematic technological requirements such as high voltage and intense magnetic fields

11

UNCLASSIFIED UNCLASSIFIED UNCLASSIFIED UL

RESEARCH SUMMARY

PROJECT TITLE:
"Dielectric Loaded Broadband Gyro-TWT System"

CONTRACT / GRANT NO.:
F49620-92-J-0175

CONTRACT / GRANT VALUE:
$89,816

CONTRACT / GRANT PERIOD OF PERFORMANCE:
Jan. 1, 1993 - Dec. 31, 1993

PRINCIPAL INVESTIGATOR:
N.C. Luhmann, Jr.

TELEPHONE NO.:
(916) 752-0360

BUSINESS MAILING ADDRESS:
Chairman, Department of Applied Science
University of California at Davis
228 Walker Hall
Davis, California 95616

RESEARCH OBJECTIVES:

Basic research studies on the generation of high frequency waves at high power, while minimizing problematic technological requirements such as high voltage and intense magnetic fields.

AFOSR PROGRAM MANAGER:
Dr. Robert Barker

PUBLICATIONS AND CONFERENCE PROCEEDINGS (1/1/93 - 12/31/93)

K.C. Leou, D.B. McDermott, F.V. Hartemann, C.K. Chong, and N.C. Luhmann, Jr., "Experimental Investigation of a Broadband Dielectric-Loaded Gyro-TWT Amplifier," submitted for publication to *Physics Review Letters*, October, 1993.

A. Gover, F.V. Hartemann, G.P. Le Sage, N.C. Luhmann, Jr., R.S. Zhang, C. Pellegrini, "Time and Frequency Domain Analysis of Superradiant Coherent Synchrotron Radiation in a Waveguide FEL," accepted for publication *Physics Review Letters.*

F.V. Hartemann, G.P. Le Sage, D.B. McDermott, N.C. Luhmann, Jr., "Coherent Synchrotron Radiation in an Ultra-Short Pulse Photocathode-Driven Waveguide Free-Electron Laser," accepted for publication *Physics Fluids B.*

K.C. Leou, D.B. McDermott, F.V. Hartemann, S.N. Fochs, and N.C. Luhmann, Jr., "Initial Operation of a Wideband Gyro-TWT Amplifier," *Technical Digest of Int. Electron Devices Meeting*, pg. 359, 1993.

G.P. LeSage, P.G. Davis, S. Fochs, F. Hartemann, D.B. McDermott, N.C. Luhmann, Jr., S.C. Hartman, S.Y. Park, R.S. Zhang, and C. Pellegrini, "Ultra-Short Pulses of Coherent Millimeter-Wave Radiation from a Prebunched FEL," submitted to *Int. Conf. on IR and Millimeter Waves*, 1993.

K.C. Leou, Q.S. Wang, C.K. Chong, A.J. Balkcum, S.N. Fochs, E. Garland, J. Pretterebner, A.T. Lin, D.B. McDermott, F. Hartemann, and N.C. Luhmann, Jr., "Gyro-TWT Amplifiers at UCLA," *Int. Conf. on IR and Millimeter Waves*, 1993.

C.K. Chong, Q.S. Wang, K.C. Leou, J.D. McNally, M.P. Bobys, A.J. Balkcum, D.B. McDermott, F. Hartemann, J. Pretterebner, A.T. Lin, and N.C. Luhmann, Jr., "High-Harmonic Gyro-Amplifiers," *Proceedings of Second Annual Vacuum Electronic Conf.*, 1993.

K.C. Leou, Q.S. Wang, C.K. Chong, A.J. Balkcum, J. Pretterebner, A.T. Lin, D.B. McDermott, F. Hartemann, and N.C. Luhmann, Jr., "Recent UCLA Fast-Wave "Amplifier Developments," *Asia-Pacific Conference*, 1, pg. 6-66, 1993.

D.B. McDermott, C.K. Chong, F.V. Hartemann, N.C. Luhmann, Jr., and A.T. Lin, " Slotted Third-Harmonic Peniotron Forward-Wave Oscillator," *Bull of Am. Phys. Society*, 38, 2001, (1993).

K.C. Leou, D.B. McDermott, F.V. Hartemann, S.N. Fochs, and N.C. Luhmann, Jr., "Dielectric Loaded Wideband Gyro-TWT," *Bull of Am. Phys. Society*, 38, 2001, (1993).

G.P. LeSage, F.V. Hartemann, P.G. Davis, S. Fochs, D.B. McDermott, N.C. Luhmann, Jr., S.C. Hartman, S. Park, R.S. Zhang, and C. Pellegrini, " Ultrashort-Pulses of Coherent Radiation in a Prebunched Free-Electron Maser," *Bull of Am. Phys. Society*, 38, 1941, (1993).

F.V. Hartemann, G.P. LeSage, S. Fochs, D.B. McDermott, and N.C. Luhmann, Jr., "Laser Ring Photocathode RF Linac," *Bull of Am. Phys. Society*, 38, 1941, (1993).

K.C. Leou, D.B. McDermott, F.V. Hartemann, S.N. Fochs, and N.C. Luhmann, Jr., "Initial Operation of a Wideband Gyro-TWT Amplifier," submitted to *SPIE Conf. on High Power Microwaves*, Los Angeles, CA, 1994.

A.T. Lin, C.K. Chong, D.B. McDermott, A.J. Balkcum, F.V. Hartemann, and N.C. Luhmann, Jr., "Slotted Third-Harmonic Peniotron Forward-Wave Oscillator," submitted to *SPIE Conf. on High Power Microwaves*, Los Angeles, CA, 1994.

OVERVIEW

During the last year, several novel millimeter-wave sources have been further developed.

(1) Stable operation of a high performance, dielectric-loaded wideband gyro-TWT has been experimentally demonstrated. For a 90 kV, 5 A, $\alpha = v_\perp/v_z = 0.6$ electron beam produced by a single-anode MIG electron gun, a peak output power of 55 kW with 11% efficiency, 27 dB saturated gain and an unprecedented constant-drive bandwidth of 11% has been achieved in the X-band frequency proof-of principle experiment.

(2) A third-harmonic slotted peniotron oscillator experiment has been built, based on Dr. A.T. Lin's recent simulation results, which predict a substantial conversion efficiency of 45%. The peniotron was designed to be driven by the same axis-encircling electron beams that are currently used to drive our third-harmonic slotted gyro-TWT amplifier.

(3) In addition, we built a high power, 35 GHz ultra-short-pulse prebunched FEL cicuit. It will be driven by the 3.5 MeV, 100 pC, 3 ps electron beam bunches produced by the X-band photocathode rf linac that we have begun to construct. The prebunched FEL is predicted to be highly efficient because all electrons in the short electron bunch give up energy to the wave. The short-pulse electron beam can thereby emit a broadband chirped ultra-short rf pulse with a center frequency exceeding 250 GHz. The first stage of the high power 100 fsec laser has been successfully tested.

A. Wideband Gyro-TWT

Future high resolution radar and high speed communication systems require wideband high power microwave or millimeter-wave amplifiers. The gyro-TWT has received considerable attention because of its high power capability. However, the constant-drive bandwidth of a conventional gyro-TWT is limited to roughly 3% due to the circuit's dispersion. Over the last two years, we have designed and constructed a gyro-TWT that was predicted to yield a significantly broader bandwidth. The features of this amplifier were described in the preceeding progress report. Its circuit had been loaded with dielectric to reduce the waveguide's dispersion so that the beam's cyclotron resonance line was tangent to an electromagnetic mode over a large frequency range. During the last year, we successfully tested this broadband gyro-TWT and achieved significant results.

A schematic of the microwave diagnostic system is shown in Fig. 1. The input rf is provided by a sweep oscillator and amplified by two cascaded helix TWT amplifiers with a minimum power of 1 kW to drive the gyro-TWT into saturation. Both the input and output rf peak powers are measured by diode detectors along with directional couplers and precision variable attenuators. The rf signal coming out of the input port is also measured with a similar setup to monitor any possible gyro-BWO type oscillations. All of the components were calibrated with an HP8510B automated network analyzer and an HP438A precision power meter, yielding an estimated accuracy of ±0.5 dB for the power measurements.

The magnetic field was adjusted to give maximum output power at 9.4 GHz and then measurements were made at other frequencies under the same operating conditions. The operating parameters are listed in Table 1. The transfer curves for the amplifier are shown in Fig. 2 for several values of beam current I_0. The small-signal dependence of gain on current fits the usual $I_0^{1/3}$ scaling. The bandwidth is shown in Fig. 3. An unprecedented constant-drive bandwidth of 11% has been achieved with a peak power of 55 kW, 11% efficiency and a saturated gain of 27 dB. By comparing to our simulation code predictions shown in Fig. 4,

the measured 11% constant-drive bandwidth implies that the electron beam has an axial velocity spread of approximately 4%. By taking the envelope of Fig. 3, the amplifier's saturated bandwidth is found to be 15%.

Of extreme importance, the amplifier was found to be stable for zero input power, which is a necessary condition for any high performance amplifier. However, oscillations in the operating mode due to both forward-wave and backward-wave interactions (gyro-BWO) could be excited separately by increasing the magnetic field. Figure 5 shows the magnetic field value at which the device becomes unstable. By digitizing the output signal, the amplifier's spectrum was found to equal the minimum transform limit for the 1.2 μs pulse. As seen in Fig. 6, the output spectrum is an accurate representation of the input signal. By mixing the output signal with the input in a double-balanced mixer, the phase stability of the amplifier was found to be 40°/kV as shown in Fig. 7.

Although the current bandwidth of 11% is quite substantial, our simulation results in Fig. 4 predict that the bandwidth can be further enhanced with improved beam quality. A 20% constant-drive bandwidth is predicted for a 2% axial velocity spread. The present design can be directly scaled to millimeter-wave frequencies. However, for high average-power applications, a corrugated metallic waveguide would be utilized. We will test such a structure in the future.

B. Third-Harmonic Peniotron

There is currently intense interest in the development of slotted high-harmonic peniotron amplifiers, because 1) peniotrons are theoretically extremely efficient, 2) harmonic operation allows the required magnetic field to be reduced significantly, and 3) the slotted circuit shown in Fig. 8 greatly ameliorates the electron energy requirement. An important issue is whether the competing gyrotron interactions will dominate and thereby degrade the desired peniotron interaction. The purpose of our slotted third-harmonic peniotron experiment is to address this issue in order to develop the harmonic peniotron into an efficient millimeter-wave source. Due to the exciting simulation results of our colleague Dr. A.T. Lin, we have modified our planned high-harmonic penio-TWT amplifier into a third-harmonic peniotron oscillator experiment. Using a PIC code and electron beam parameters that are readily accessible to our test-stand, Dr. Lin found that a third-harmonic peniotron in an 8-vane travelling-wave circuit could yield an efficiency of 45% if the third-harmonic cyclotron resonance line intersects the π-mode at its cutoff frequency. Although gyrotron interactions usually dominate, the peniotron interaction dominates this new system due to the nonresonant matched circuit, where interactions near their cutoff are emphasized, and extremely high efficiency is obtained. Figure 9 shows the growth in time and space of the 45% efficient, third-harmonic peniotron studied by Dr. Lin. It is evident that the excited wave travels in the same direction as the electron beam. The competing gyrotron interaction remains at a low level. An interesting question that we will experimentally address is raised by Dr. Lin's simulation result: What produces the necessary feedback in this oscillator where the wave and beam travel in the same direction?

We have built an 8-vane third-harmonic peniotron experiment, which uses the electron beam and circuit parameters from Dr. Lin's simulation. The circuit was fabricated by electric discharge wire machining. The design parameters are listed in Table 2. A schematic of the circuit is shown in Fig. 10. So that the interaction structure is a nonresonant, travelling-wave circuit, it is crucial that it be terminated at both ends. The electron gun end of the circuit is an attenuator formed by placing lossy dielectric wedges in the slots. On the collector end, the circuit tapers into a four-period, beat-wave mode

converter which transforms the TE_{41} mode into the more useful TE_{11} mode. The measured behavior of this converter is shown in Fig. 11. The TE_{11} wave is then transformed into the common TE_{10} fundamental mode of rectangular waveguide and then into either a transmitting antenna or a load.

The peniotron will be driven by the axis-encircling electron beams produced by our high current gyroresonant rf accelerator. Since the beam parameters for the experiment (Table 2) are the same as used in our current rf-accelerated, third-harmonic slotted gyro-TWT amplifier experiment, the same accelerator cavity will be used. The acceleration characteristics of the TE_{111} cavity are shown in Fig. 12. The slotted peniotron experiment will be performed after the slotted gyro-TWT experiment has been concluded. The performance of the third-harmonic peniotron will be compared to the behavior of the third-harmonic gyro-TWT.

C. Ultra-Short-Pulse Prebunched FEL

Ultra-short, high-power pulses of coherent submillimeter-wave radiation have numerous applications, ranging from surface and material physics to the next generation of ultra-wideband radars. We have begun to develop a source that will generate an extremely short pulse wave. It is driven by an electron beam created in a photocathode rf linac, where the beam's pulsewidth is determined by the pulsewidth of the laser. The short-pulse electron beam then efficiently transfers its energy in a prebunched FEL interaction. Since the width of the beam is much shorter than the wavelength of the generated wave, all electrons are in a decelerating phase and lose energy. The 100 μm width photo-electron beam from a 100 fsec Ti-sapphire laser (frequency multiplied to the UV) can thereby be used to emit a broadband chirped ultra-short rf pulse with a center frequency exceeding 250 GHz. For highly efficient conversion, the FEL wiggler should be tapered in the saturation region.

We have begun to construct a photocathode rf linac. A schematic of the setup is shown in Fig. 13. The aluminum photocathode will be excited by a self mode-locked, externally phase-locked, 100 fs, 100 mJ, frequency-tripled UV Ti:Sapphire laser. The first stage of the laser has already been successfully tested. The linac will be driven by our 20 MW, 8.568 GHz SLAC klystron. The klystron's modulator has been used previously. A special feature of this novel rf gun is that the photocathode is also a mirror in a ring-resonator so that the quantum efficiency of the photocathode is enhanced by multiple passes of the UV radiation. A train of electron micropulses will be created rather than just one pulse.

We have developed a linear theory of the prebunched FEL interaction. The analysis is appropriate for an interaction either in free-space or in waveguide. For a point charge and a free-space interaction in a twenty period wiggler, the normalized frequency spectrum is shown in Fig. 14. The spectrum is similar to that from a conventional non-prebunched FEL. However, the amplitude is orders of magnitude higher. Figure 15 shows the predicted fall-off of the output power as the bunch width Δz becomes comparable to the wavelength. For a grazing intersection between the beam and wave, there is no slippage between them and the width of the wave-packet is determined by the transform limit of the FEL bandwidth and the dispersion of the waveguide. The output pulsewidth of 50 ps predicted for our 35 GHz, proof-of-principle experiment is shown in Fig. 16.

The experiment was designed for a grazing interaction. The parameters for the experiment are listed in Table 3. The tapered 3 kG, pulsed helical wiggler with a period of 8.4 cm and a length of 2 m was tested and the field component in one plane is shown in Fig.

17. Several diagnostics have been assembled. A fluorescent glass Faraday Cup will allow the measurement of the time-integrated beam current. The 35 GHz output power will be measured by using a calibrated Ka-band pick-up probe and a series of long waveguide attenuators. The 40-60 GHz waveguide will also be used as a dispersive delay line to expand the ~50 ps broadband pulse to a more measurable 10 ns. A Ka-band interferometer will be used to view the actual pulsewidth.

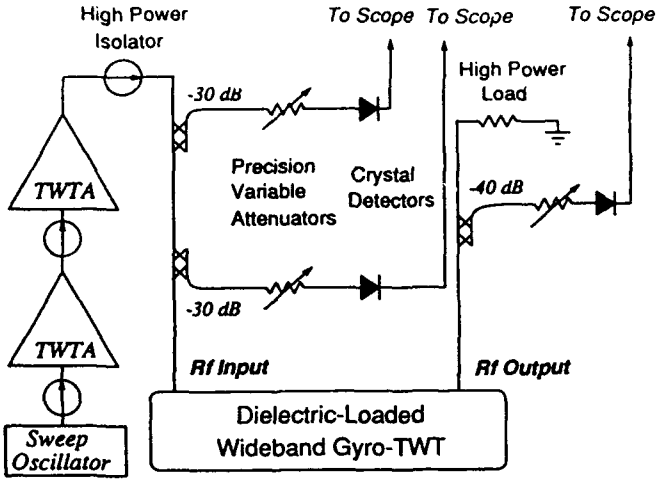

Figure 1. Schematic of the external rf system for the wideband gyro-TWT amplifier.

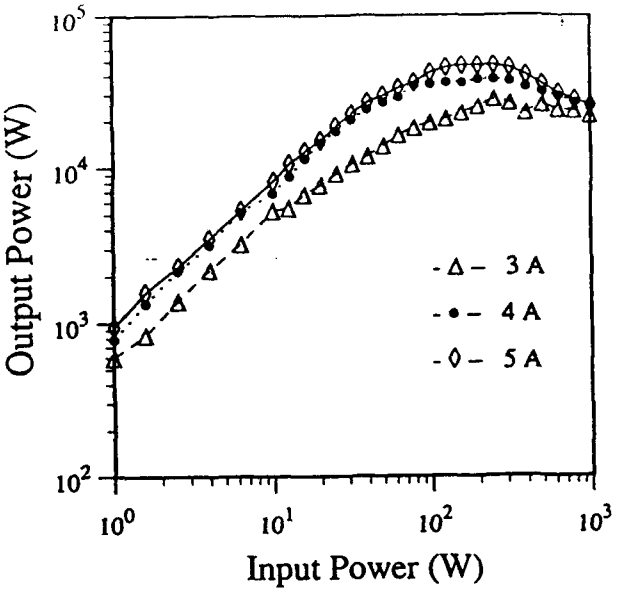

Figure 2. Measured dependence of output power on input power for three values of electron beam current in wideband gyro-TWT amplifier.

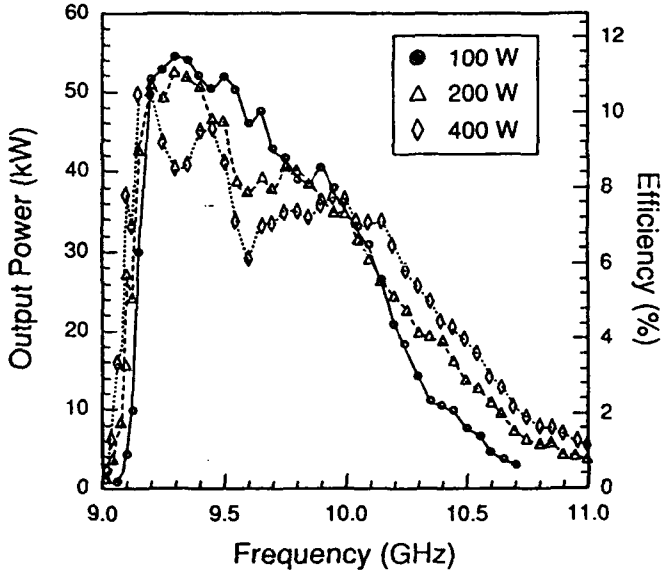

Figure 3. Measured dependence of output power on frequency for three values of input power.

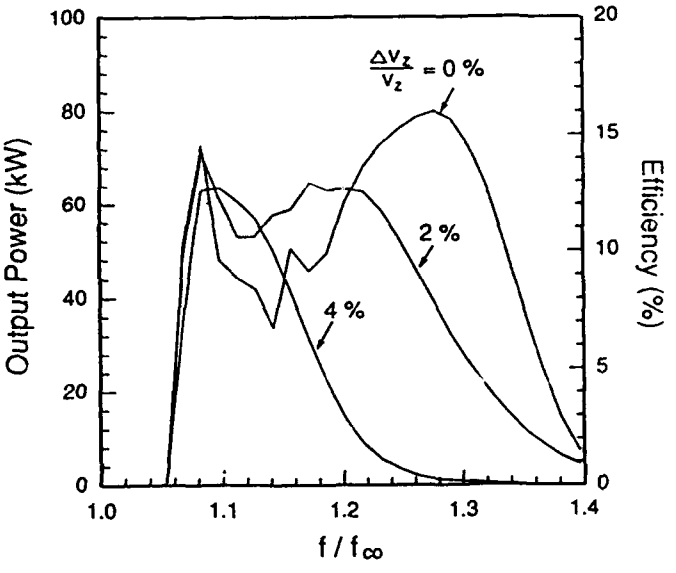

Figure 4. Predicted dependence of output power and efficiency on frequency for several values of axial velocity spread (P_{in} = 100 W).

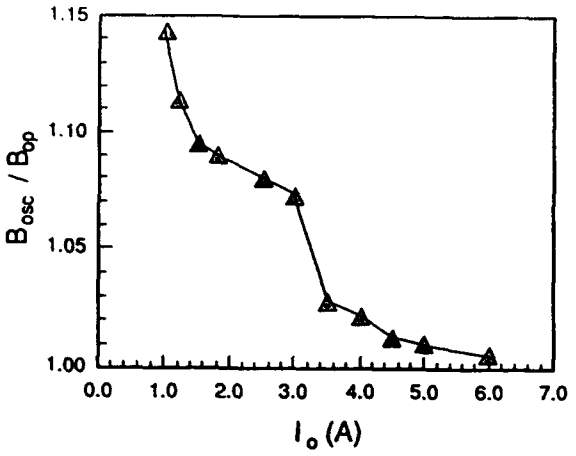

Figure 5. Measured dependence on beam curent of minimum magnetic field (normalized to operating field) for onset of absolute instability.

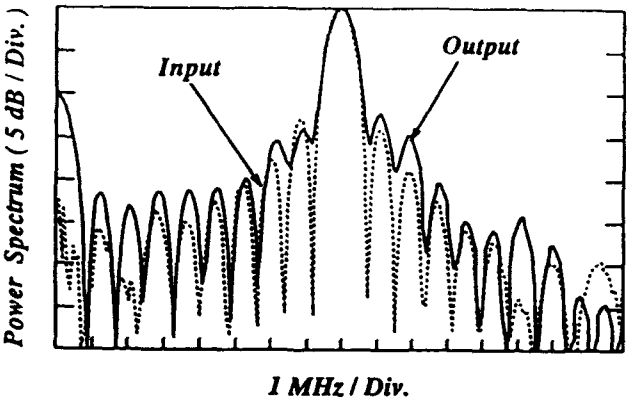

Figure 6. Measured spectrum of the 1.2 μs pulse input and output 9.4 GHz rf signals.

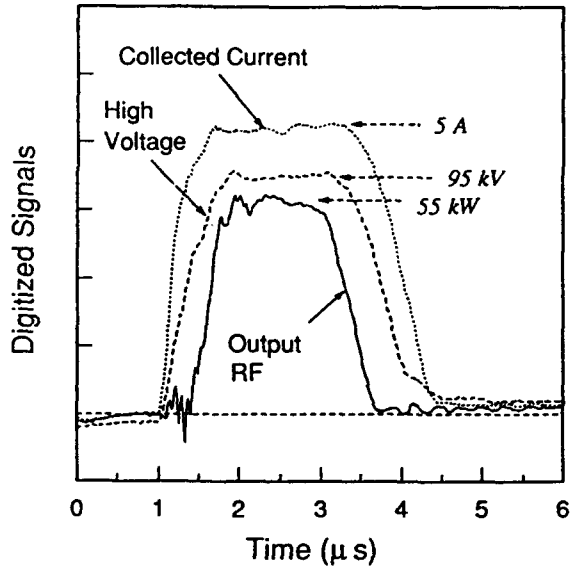

Figure 7. Temporal dependence of high-voltage pulse, rf output pulse, in-quadrature and out-of-quadrature signals from double-balanced mixing of the input and output rf signals.

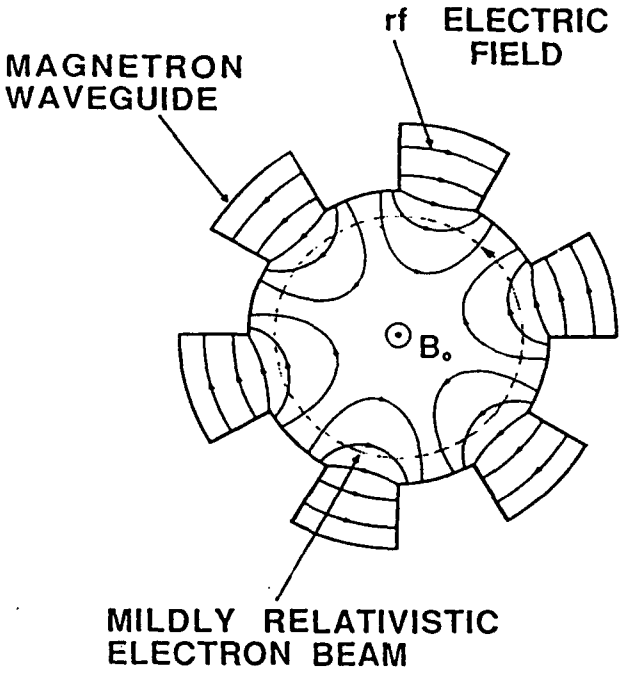

Figure 8. Cross-sectional view of a slotted second-harmonic peniotron-TWT with six vanes and showing the rf electric field pattern of the π mode.

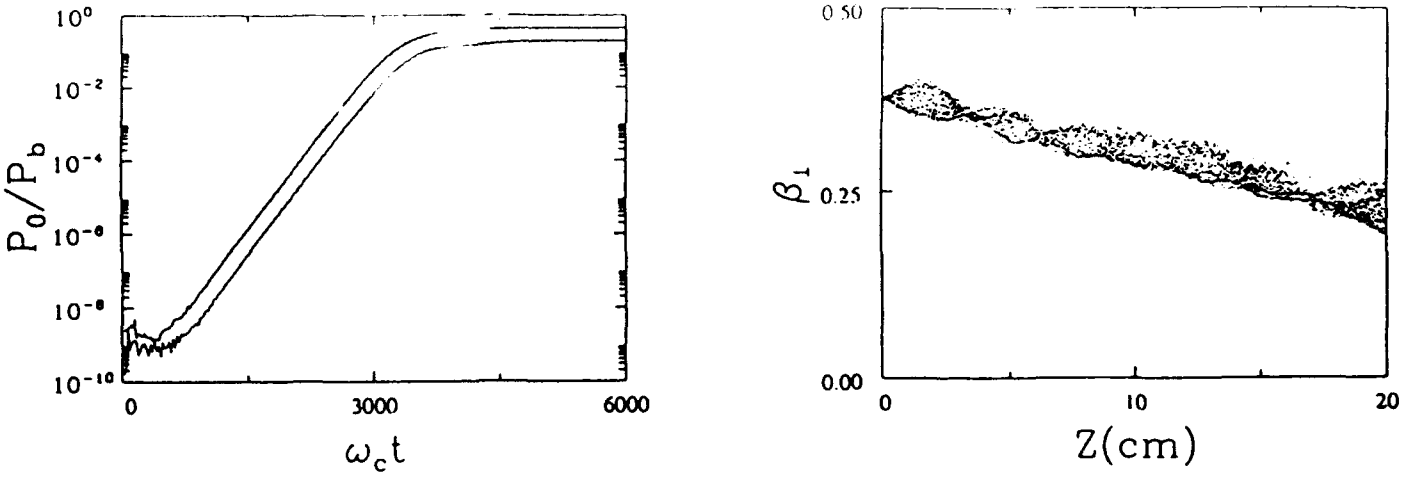

Figure 9. PIC simuation results from Dr. A.T. Lin of slotted third-harmonic peniotron (Table 2), showing (a) temporal dependence of output power normalized to the beam power and (b) spatial dependence of transverse velocity during saturation at $\Omega_c t = 4000$.

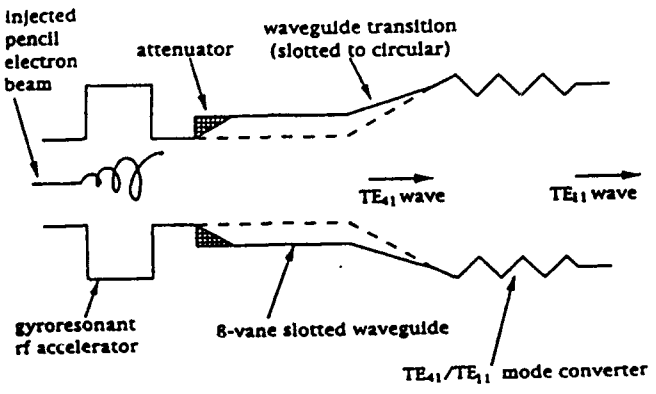

Figure 10. Schematic of slotted third-harmonic peniotron forward-wave oscillator proof-of-principle experiment.

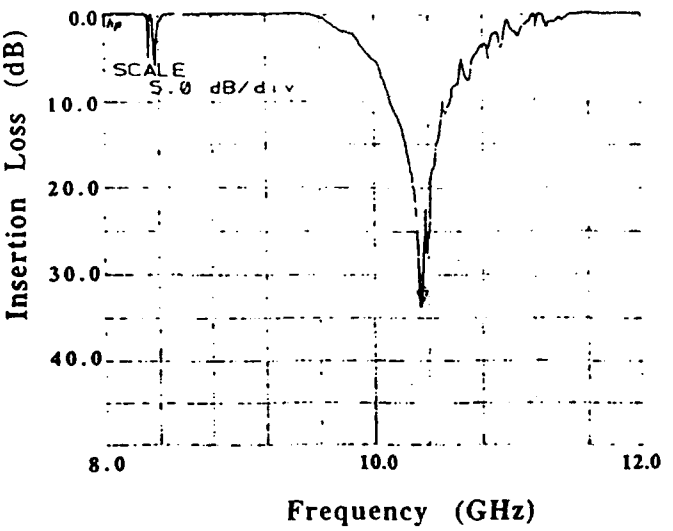

Figure 11. Bandwidth measurement from network analysis of power remaining in TE_{11} mode for TE_{11} wave injected into four-period TE_{41}/TE_{11} beat-wave mode converter.

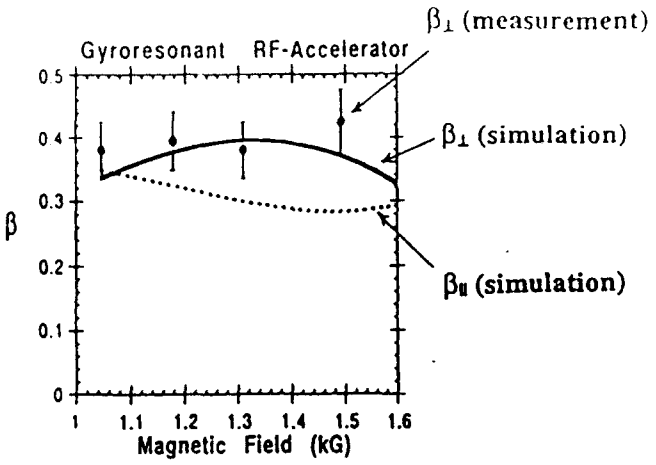

Figure 12. Dependence on magnetic field of transverse and axial velocity (normalized to the speed of light) from gyroresonant rf accelerator with P_{in} = 1 MW and L/r_w = 0.92 from simulation (curves) and measurement (filled circles).

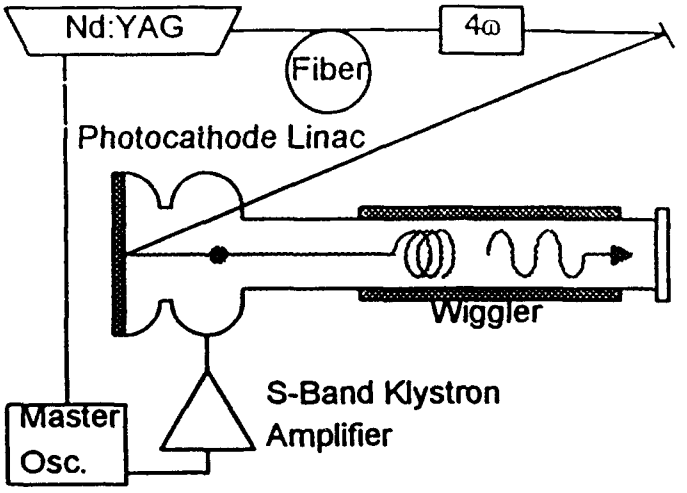

Figure 13. Schematic of prebunched FEL experiment driven by a photocathode rf linac.

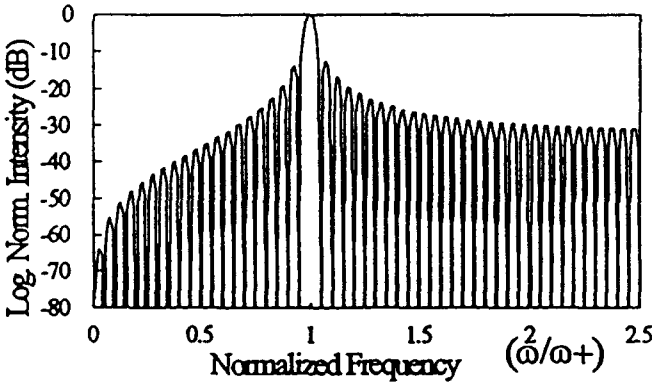

Figure 14. Predicted on-axis spectrum from proposed prebunched FEL (Table 3 with $\omega_c=\infty$).

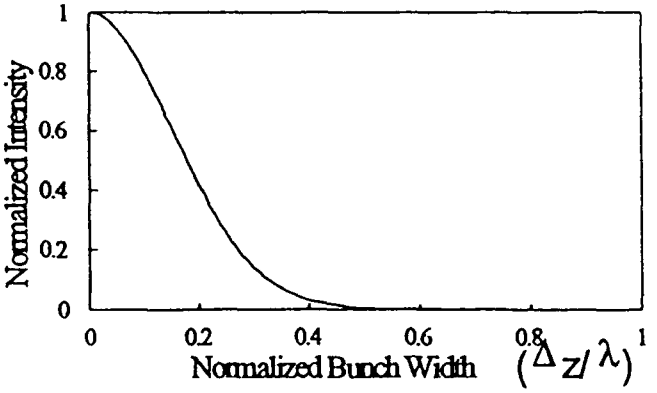

Figure 15. Predicted dependence of output power on bunch width Δz normalized to output wavelength from proposed prebunched FEL (Table 3 with $\omega_c=\infty$).

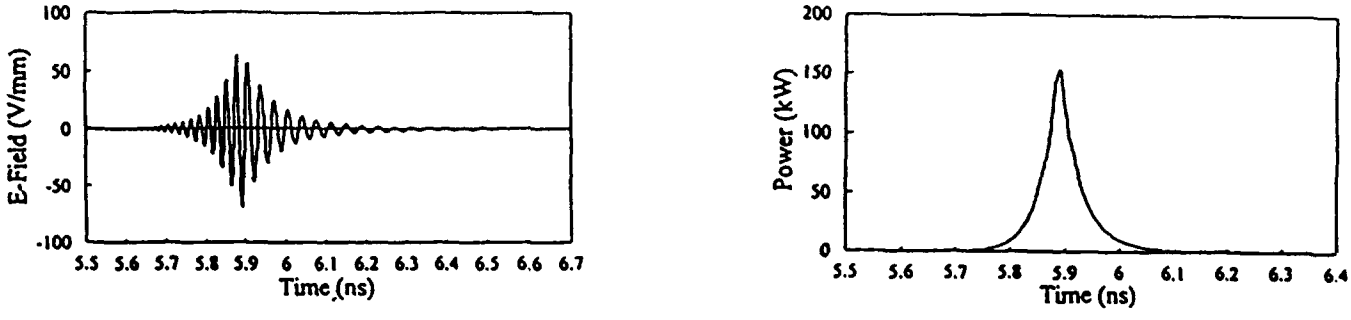

Figure 16. Predicted temporal dependence of output rf pulse's (a) field and (b) power from proposed prebunched grazing FEL (Table 3).

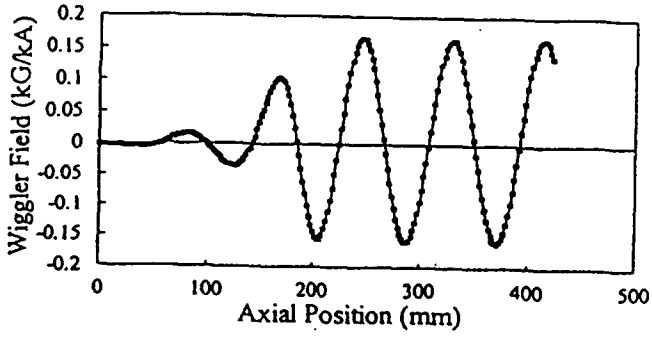

Figure 17. Measured axial dependence of helical wiggler's magnetic field component in plane through the axis.